HHS Public Access

Author manuscript

Phytother Res. Author manuscript; available in PMC 2022 November 01.

Published in final edited form as:

Phytother Res. 2021 November ; 35(11): 6255–6269. doi:10.1002/ptr.7271.

Peonidin-3-O-glucoside and cyanidin increase osteoblast differentiation and reduce RANKL-induced bone resorption in transgenic medaka

Zhitao Ren[1,2], **Nishikant A. Raut**[3,4], **Temitope O. Lawal**[5,6], **Shital R. Patel**[1], **Simon M. Lee**[2], **Gail B. Mahady**[1]

[1]Department of Pharmacy Practice, College of Pharmacy, WHO Collaborating Centre for Traditional Medicine, University of Illinois at Chicago, Chicago, Illinois

[2]State Key Laboratory of 0051uality Research in Chinese Medicine and Institute of Chinese Medical Sciences, University of Macau, Macau, China

[3]Raman Fellow, Department of Pharmacy Practice, College of Pharmacy, WHO Collaborating Centre for Traditional Medicine, University of Illinois at Chicago, Chicago, Illinois

[4]Department of Pharmaceutical Sciences, Rashtrasant Tukadoji Maharaj Nagpur University, Nagpur, India

[5]Schlumberger Fellow, Department of Pharmacy Practice, College of Pharmacy, WHO Collaborating Centre for Traditional Medicine, University of Illinois at Chicago, Chicago, Illinois

[6]Department of Pharmaceutical Microbiology, University of Ibadan, Ibadan, Nigeria

Abstract

Experimental and clinical studies suggest a positive impact of anthocyanins on bone health; however, the mechanisms of anthocyanins altering the differentiation and function of osteoblasts and osteoclasts are not fully understood. This work demonstrates that dietary anthocyanins and resveratrol increased proliferation of cultured human hFOB 1.19 osteoblasts. In addition, treatment of serum starvation of hFOB osteoblasts with anthocyanins and resveratrol at 1.0 μg/ml reduced apoptosis, the Bax/Bcl-2 ratio, p53, and HDAC1 expression, but increased SIRT1/3 and PGC1α mRNA expression, suggesting mitochondrial and epigenetic regulation. In *Sp7/osterix*:mCherry transgenic medaka, peonidin-3-O-glucoside and resveratrol increased osteoblast

Correspondence Nishikant A. Raut, Raman Fellow, Department of Pharmacy Practice, College of Pharmacy, WHO Collaborating Centre for Traditional Medicine, University of Illinois at Chicago, Chicago IL 60612, USA & Department of Pharmaceutical Sciences, Rashtrasant Tukadoji Maharaj Nagpur University, Nagpur, India. nishikantraut29@gmail.com.

AUTHOR CONTRIBUTIONS

ZR and NAR performed the experimental work related to the medaka fish, SRP and TOL have performed the experimental work related to hFOB cells, GBM and SML conceptualized, planned, and supervised the experimental work, analyzed the data, wrote, and finalized the manuscript.

CONFLICT OF INTEREST

The authors declare no conflicts of interest.

DATA AVAILABILITY STATEMENT

The data that support the findings of this study are available from the corresponding author upon reasonable request.

SUPPORTING INFORMATION

Additional supporting information may be found in the online version of the article at the publisher's website.

differentiation and increased the expression of *Sp7/osterix*. Cyanidin, peonidin-3-O-glucoside, and resveratrol also reduced RANKL-induced ectopic osteoclast formation and bone resorption in *col10a1*:nlGFP/*rankl*:HSE: CFP medaka in doses of 1–4 μg/ml. The results indicate that both cyanidin and peonidin-3-O-glucoside have anabolic effects on bone, increasing osteoblast proliferation and differentiation, mitochondrial biogenesis, and by altering the osteoblast epigenome. Cyanidin and peonidin-3-O-glucoside also reduced RANKL-induced bone resorption in a transgenic medaka model of bone resorption. Thus, peonidin-3-O-glucoside and cyanidin appear to both increase bone formation and reduce bone loss, suggesting that they be further investigated as potential treatments for osteoporosis and osteomalacia.

Keywords

apoptosis; cyanidin; osteoblasts; osteoclast; osteoporosis; p53; peonidin; RANKL; resveratrol; SIRT1

1 | INTRODUCTION

Bone remodeling disorders impact millions of patients annually, causing significant morbidity and mortality (Appelman-Dijkstra & Papapoulos, 2018; Feng & McDonald, 2011; McGowen et al., 2004; Sozen et al., 2017). Osteoporosis, the most common bone remodeling disorder is caused by an imbalance between bone resorption and formation, and leads to greater risk of fragility fractures (Appelman-Dijkstra & Papapoulos, 2018; Feng & McDonald, 2011). More than 200 million people worldwide are affected by osteoporosis and osteopenia, and these diseases are increasingly becoming global epidemics (Chang et al., 2017; Qaseem et al., 2017). According to statistical data from the International Osteoporosis Foundation, one in three women and one in five men >50 years old have a higher risk of osteoporotic fractures in their lifetime, affecting their health, independence, and productivity (IOF, 2017). In addition, other less common, but also important, disorders of bone remodeling include Paget's disease, bone loss associated with alcohol consumption, osteopetrosis, renal osteodystrophy allied with dialysis therapy and non-inherited (dietary) rickets (rare) (Feng & McDonald, 2011; McGowen et al., 2004; Sozen et al., 2017).

Bone remodeling is a tightly coordinated process involving the removal of old bone by osteoclasts through bone resorption, and formation of new bone by osteoblasts (Appelman-Dijkstra & Papapoulos, 2018; Feng & McDonald, 2011; Haas & LeBoff, 2018; McGowen et al., 2004; Sozen et al., 2017). Proper functioning of bone remodeling is key for maintaining the strength and integrity of bone. In age-related bone loss and osteoporosis, there is a characteristic increase in osteoclast formation and bone resorption, as well as an increase in osteoblast apoptosis and reduced bone formation (Manolagas, 2010). In the past, the treatment of osteoporosis and other related diseases has focused on the inhibition of osteoclastogenesis, and very few treatments have been directed toward increasing bone formation (Raut et al., 2019). While anti-resorptive agents are effective for improving bone mass, they also are associated with serious adverse events, including atypical femoral fractures, dementia, hypocalcemia, increased risk of coronary heart disease, osteonecrosis of the jaw, upper gastrointestinal symptoms, and stroke (Kanis et al., 2013; Qaseem et al.,

2017; Rossini et al., 2016). Thus, future treatments should focus not only on reducing bone loss but also on improving bone mass. Considering there is a lack of drugs available that have both bone-resorbing and bone anabolic activities, naturally occurring compounds are being extensively investigated as safer alternatives to bone remodeling therapies (Sakaki et al., 2018).

While several natural products and isolated phytoconstituents are reported to have beneficial effects in bone diseases, only resveratrol, specific phenolic acids, and dietary anthocyanins have been reported to inhibit bone resorption and increase bone formation through epigenetic mechanisms of action (Danks et al., 2016; He et al., 2015; Mizutani et al., 1998; Raut et al., 2019; Su et al., 2018). For example, resveratrol, one of the most intensively investigated natural compounds, has numerous pharmacological activities, including treatment for cancer, cardiovascular, diabetes, inflammatory, and osteoporosis (Raut et al., 2019). Studies have shown that resveratrol increased the expression of bone morphogenetic protein 2 (BMP-2) and reduced bone loss in ovariectomized rats (Mizutani et al., 1998; Su et al., 2018). Resveratrol further reduced apoptosis in cultured mouse osteoblasts by activating SIRT1 and suppressed bone resorption in an osteoporosis model by inhibiting the expression of nuclear factor kappa-β ligand (RANKL) (Mizutani et al., 1998). Thus, in this study, we have used resveratrol as a positive control comparison compound.

Anthocyanins are naturally occurring water-soluble pigments found in food plants such as grapes and berries and possess numerous pharmacological activities with beneficial effects against atherosclerosis, cancer, cardiovascular disease, and diabetes (Hou et al., 2003; Jayaprakasam et al., 2005). More recently, anthocyanins, such as delphinidin and cyanidin, have been reported to prevent bone resorption (Imangali et al., 2020; Lee et al., 2014, 2015; Moriwaki et al., 2014) and protect against obesity and oxidative stress-induced bone loss in mice (Cheng et al., 2018; Lee et al., 2014). However, the effects of ACNs on osteoblastogenesis, as well as their cellular and molecular mechanism(s), remain poorly understood (Cheng et al., 2018).

The aims of the study were to investigate the effects, as well as cellular and molecular mechanisms of dietary anthocyanins in human hFOB 1.19 osteoblasts and novel double transgenic medaka (*Oryzias latipes*) models of bone development and osteoporosis, to determine the effects of these compounds on osteoblast proliferation and apoptosis, and RANKL-induced osteoclastogenesis and bone resorption.

2 | MATERIALS AND METHODS

2.1 | Cell culture and maintenance

The human osteoblast cell line, hFOB 1.19 (ATCC® CRL-11372™), was purchased from American Type Cell Culture, ATCC (Manassas, VA). hFOBs are a homogeneous, rapidly proliferating cell line that allows for the study of normal human osteoblast differentiation, osteoblast physiology, and determine the effects of compounds on osteoblast apoptosis, proliferation, function, and differentiation. The hFOB 1.19 osteoblasts were cultured in a 1:1 mixture of Ham's F12 medium and Dulbecco's Modified Eagle's medium, with 2.5 mM L-glutamine (without phenol red). For the complete growth medium, 0.3 mg/ml G418 and

fetal bovine serum (FBS, 10%) were added to the base media (ATCC, Manassas, VA). To subculture, the culture medium was removed, and the cell layer was rinsed with 0.25% (w/v) Trypsin 0.53 mM EDTA solution for 5–15 min, and the 6.0–8.0 ml of complete growth medium and cells were aspirated by gently pipetting. Aliquots of the cell suspension were transferred to new culture vessels and incubated at 34°C. Media were renewed every 2–3 days at 5% CO_2 atmosphere. Harvesting of cells at 80–90% confluency was performed with addition of 0.25% trypsin/EDTA and counted using Trypan blue and hemocytometer. The cells were re-suspended in growth medium at appropriate density and plated for performing cellular assays. For serum starvation, the cells were cultured in media without FBS for 24 hr before the addition of the compounds.

2.2 | Cell treatment and viability assay

Four pure ACNs (cyanidin, CYN; peonidin-3-O-glucoside, POG; delphinidin, DC; delphinidin-3-glucoside, DGC) and resveratrol (RES) purity >95% were obtained from Polyphenols, Sandes Norway and analyzed for quality and stability by Q-TOF LC–MS as described (Mulabagal et al., 2012). The seeding of hFOB osteoblasts in triplicate was done in opaque-walled 96-well plate at 5×10^4 cells in 100 μl/well and left overnight to attach to the plate. Culture medium in the wells was replaced with fresh medium and resveratrol or the four ACNs at concentrations of 1–20 μg/ml were added to experimental wells. Vehicle (0.01% DMSO) cell control was prepared and the plates were allowed to incubate for 72 hr at 34°C in a humidified incubator. After 72 hr of incubation, a 100 μl of CellTiter-Glo® 2.0 Reagent (Promega Corporation, Madison, WI) was added in each well and treated according to manufacturer's instructions. Synergy HT plate reader (Biotek, Winooski, VT) and Gen5 1.11 software were used to read luminescence signal. The EC_{50} was defined as the concentration that causes 50% inhibition or increase of cell proliferation after exposure to extracts for 72 hr. Cell viability assays were tested in triplicates for each concentration of the partitions in two independent experiments ($n = 6$).

2.3 | Caspase-Glo® 3/7 and Caspase-Glo® 8 apoptosis assays

Serum-starved hFOB cells were seeded in 100 μl/well in opaque-walled 96-well plates in triplicate at a density of 5×10^4 cells and incubated overnight. Anthocyanins in sterile water in concentrations of 1–20 μg/ml were added to the test wells. Caspase-Glo® 3/7 and 8 reagents (all Promega Corporation, Madison, WI) were prepared following the manufacturer's instructions and allowing it to equilibrate to room temperature. After 6 hr of incubation, the control and test plates containing treated cells were removed from the incubator to equilibrate them to room temperature. Caspase-Glo® 3/7 or 8 reagents, each of 100 μl, were added to every well containing 100 μl of blank, negative control and treated cells in culture medium in a 96-well plate. In order to ensure uniform mixing, the plates were shaken for 30 s at 300–500 rpm, employing a plate shaker and incubated for 2 hr at room temperature. Synergy HT plate reader (Biotek, Winooski, VT) and Gen5 1.11 software were used to read the luminescence of each sample.

2.4 | RNA isolation

The seeding of hFOB osteoblasts in triplicate was done in a 6-well plate at a density of 1.2×10^6 cells/ml and incubated overnight. Cells were treated with ACNs at 1 μg/ml,

and after 6 hr, total RNA was extracted from cells using Trizol (ThermoFisher Scientific, Waltham, MA) following the manufacturer's instructions. Vehicle solvent (negative control) treated cells were included. Synergy HT Take 3 session (Biotek, Winooski, VT) and Gen5 1.11 software were used to determine the concentration and quality of isolated RNA by measuring absorbance at 260 and 280 nm.

2.5 | Quantitative polymerase chain reaction

Power SYBR Green RNA-to-CT 1-step kit (Applied Biosystems, Foster City, CA) was used to reverse transcribe and amplify the total RNA according to manufacturer's instructions employing the StepOne Plus Real-Time PCR System (Applied Biosystem, Foster City, CA). Primer sequences reported in the literature were selected (Mulabagal et al., 2012). β-actin was used as the endogenous control (Haas & LeBoff, 2018). Briefly, each of the polymerase chain reaction was carried out in a volume of 10 μl by mixing 100 ng RNA, RT Enzyme Mix (125×), 200 nM of each primer and Power SYBR Green RT-PCR Mix (2×) performing it in duplicate. The cycling conditions include 48°C for 30 min followed by 95°C for next 10 min to start 50 cycles of 95°C maintained for 15 s and 60°C maintained for 1 min by confirming the specificity of PCR reaction by melt curve analysis at 95°C for 15 s, 60°C for 15 s, and 95°C for 15 s.

The gene expression was quantified using endogenous control β-actin gene and using the ΔΔCT calculation comparing it to the calibrator (control cells). Other primers used in this study were as follows (Chen et al., 2014; Liu & Bodmer, 2006; Ouaïssi et al., 2014; Scarpulla, 2011; Solomon et al., 2018):

2.6 | Western blot analysis

The hFOB human osteoblasts were harvested from 6-well plates, and lysis was performed using 1 ml of lysis buffer comprising 10 mmol/1 Tris–HCl of pH 7.9, 3 mmol/1 $MgCl_2$, 1% NP-40, and 10 mM/1 NaCl for 4 min on ice, then centrifuging it for 10 min at 3000 g. The pellets obtained after centrifugation were again suspended in 50 μl of extraction buffer comprising 20 mM/1 HEPES of pH 7.9, 1.5 mM/1 $MgCl_2$, 20% glycerol, 0.2 mM/1 EDTA, 1 mM/1 PMSF, and 1 mM/1 DTT followed by incubating it for 30 min and finally centrifuged at 13,000 g. Protein concentrations were measured using the Bradford assay (ThermoFisher Scientific, St Louis, MO) and supernatants were preserved at −70°C. For the western blot analysis, 40 μg of protein extracts were separated by 10% SDS-polyacrylamide gel electrophoresis and transferred to a polyvinylidene difluoride membrane (Millipore Corp., Bedford, MA), then incubated with anti-SIRT1 (mouse monoclonal antibody; 1:1,000; Cat. No. 8469), acetylated-p53 (Lys382; rabbit polyclonal antibody; 1:1,000; Cat. No. 2525), p53 (rabbit monoclonal antibody; 1:1,000, Cat. No. 2527) (Cell Signaling technology, Inc., Danvers, MA), and anti-β-actin (mouse monoclonal antibody; 1:500; Santa Cruz Biotechnology, Inc., Santa Cruz, CA) antibodies at 40°C for 24 hr. The blots were developed using a chemiluminescent substrate kit (Pierce Biotechnology, Inc., Rockford, IL). The intensity of the bands was detected and analyzed using a Quantity One analyzing system (Bio-Rad Laboratories, Inc., Hercules, CA).

2.7 | Medaka maintenance and treatment

Double transgenic *Sp7/osterix*:mCherry medaka were housed and maintained in the Biological Resource Center (the Animal Care facility at UIC under approved ACC protocol 17–166). The medaka were housed in Pentair Aquatic Eco-Systems Z-hab mini aquatic research habitat, with 32 tanks. In these medaka, early bone formation regions show good expression of *Sp7/osterix*, which remained highly expressed in bone matrix mineralized by mature osteoblasts (Imangali et al., 2020; Renn & Winkler, 2009; Yu & Winkler, 2017). The *Sp7/osx*:mCherry transgenic medaka express mCherry under control of the *Sp7/osx* promoter that is exclusively expressed in osteoblast precursors and mature osteoblasts and has been previously described in detail (Imangali et al., 2020; Renn & Winkler, 2009; Yu & Winkler, 2017). Non-invasive live quantitative fluorescence imaging and analysis of osteoblasts in these transgenic medaka is possible over a wide-range of life stages from larvae to adulthood. All medaka lines were maintained under a photoperiod of 14 hr light/10 hr darkness at 28°C as we have described (Imangali et al., 2020). Embryos were maintained in 0.3× Danieau's solution (0.23 mM KCl, 19.3 mM NaCl, 0.2 mM $Ca[NO3]_2$, 0.13 mM $MgSO_4$ and 1.7 mM HEPES, pH 7.0) at 30°C after collection and staged as described (Imangali et al., 2020). To ensure normal development of the embryos, the maintenance medium was replaced daily and from 5 dpf onwards embryos were inspected for expression of fluorescence reporter. Until 14 dpf, hatchlings were maintained at 30°C while, 14 dpf onwards at 26°C. In vivo imaging of *Sp7/osx*:mCherry transgenic fish allows us to quantitatively determine osteoblast differentiation and correlate these data with bone mineralization, as well as the molecular and epigenetic mechanisms that control osteoblast differentiation and maturation. The expression of extracellular matrix proteins supporting adhesion, proliferation, differentiation, and migration of osteoblasts in the bone microenvironment has been regulated by Runx2 and *Sp7/osx* during the progress of maturation of osteoblasts. Thus, these transgenic lines allow us to perform in vivo quantitative analysis of osteoblasts during wide-ranging stages, including mesenchymal progenitor, osteoblast progenitor, and immature to mature osteoblasts over a variety of life stages in these fish.

To investigate the effects of resveratrol and ACNs on RANKL-induced bone resorption, we used double transgenic *col10a1*: nlGFP/*rankl*:HSE:CFP medaka. In this transgenic line, the osteoblasts express nlGFP (green fluorescent protein) under control of the *col10a1* promoter and show the origin and behavior of *col10a1* positive cells during notochordal sheath mineralization in vivo (Renn & Winkler, 2010). Bone matrix molecules consisting of collagenous proteins, including collagen type X alpha 1 and collagen type I alpha 1, as well as non-collagenous proteins such as osteocalcin, osteonectin, and osteopontin provide the structural support for bone. While *col10a1* is a marker for hypertrophic chondrocytes in birds and mammals, in medaka, the expression of *col10a1* occurs in early osteoblasts (osteoblast progenitors) prior to mineralization and partially overlaps with the expression of *Sp7/osx* (Renn & Winkler, 2010). The *col10a1*:nlGFP/*rankl*:HSE:CFP medaka also overexpress RANKL after heat-shock induction inducing a strong osteoporosis-like phenotype with the formation of ectopic osteoclasts severe degradation of newly mineralized matrix in the vertebral column and other bone structures (Imangali et al., 2020). RANKL induction was achieved by heat shock at 39°C for 1.5–2 hr of the *col10a1*:nlGFP/

rankl:HSE:CFP larvae at 9 dpf. After heat shock, larvae were allowed to recover for 1 hr at 30°C and then screened for the expression of cyano-fluorescent protein (CFP), which indicates successful RANKL induction. In order to assess the effect of drug treatment, larvae that have shown expression of both CFP and *col10a1*:nlGFP were selected and housed in six-well plates (six larvae per well). Resveratrol and anthocyanins, by dissolving in fish medium, in doses of 1–10 μg/ml were added in the respective wells for 5 days after heat shock. Control larvae (+RANKL, non-drug-treated) after heat shock received no heat shock (−RANKL, non-drug treated control), and no heat shock (−RANKL, drug treated control) were maintained in fish medium by replacing fresh media daily.

2.8 | Live and fixed bone staining

For live staining, treated larvae were immersed into the staining solution of 0.1% Alizarin Complexone (alizarin-3-methyliminodiacetic acid, ALC) as described (Imangali et al., 2020) or 0.01% calcein, and all dyes were dissolved in the fish medium. The larvae (at 9–15 dpf) were incubated in the staining solution for 1.5 or 2.5 hr at 30°C followed by analysis of staining by means of tetramethylrhodamine (TRITC) and GFP filter settings. Fixed staining was performed using Alizarin Red in fixed medaka larvae as we have described (Imangali et al., 2020; Renn & Winkler, 2009).

2.9 | Live imaging

In vivo fluorescence imaging of live medaka was performed as we have previously described (Imangali et al., 2020; Renn & Winkler, 2009). Briefly, the viability and gross morphological changes in transgenic medaka after treatments were observed under a microscope (Olympus MVX10, Japan and ColorView II, Soft Imaging System, Olympus) after anesthetization with 0.02% tricaine. Fluorescence and confocal imaging were performed using an Olympus fluorescence microscope and a Zeiss Big confocal microscope at 4x magnification and 250 resolution. The images were analyzed using ImageJ, ACDSee 7.0, and Adobe Photoshop 7.0, which are quantitative and can measure regions of interest (ROIs) using ImageJ (NIH) and the add-on-ROI manager. Measuring exact ROIs, using the same exact size, exposure, and position, provides a fluorescence output value that is quantitative.

2.10 | Statistics

Differences between hFOB cell treatments and gene expression are presented as means ± SD. One-way ANOVA followed by Dunnett's or Tukey's multiple comparison tests were used to compare the differences between the groups. A p value <0.05 was considered as statistically significant. Analyses of the medaka larvae with the correct phenotype were recorded. Analysis of fluorescence imaging and density were assessed using ImageJ and the ROI manager. Results were expressed as percentages with mean ± SD using GraphPad/Prism 8.2. For comparing the groups individually and determining the significance, two-tailed Student's t-test was employed. $*p < 0.05$, $**p < 0.01$, $***p < 0.001$, and $****p < 0.0001$ were considered statistically significant.

3 | RESULTS

3.1 | Peonidin-3-O-glucoside and resveratrol increase the proliferation and differentiation of cultured human hFOB 1.19 osteoblasts

Cultured hFOB osteoblasts grown in media containing 10% FBS were treated with resveratrol (RES), delphinidin-3-O-glucoside (DGC), delphinidin (DC), cyanidin (CYN), and peonidin-3-O-glucoside (POG) at a concentration of 1 μg/ml for 72 hr (Figure 1a). Vehicle control cells were treated with 0.01% DMSO. Both RES (****$p < 0.0001$) and POG (***$p < 0.001$) significantly increased osteoblast viability and proliferation above controls, while DC, DGC, and CYN were not active up to 10 μg/ml (Figure 1a). Both resveratrol and peonidin-3-O-glucoside increased the proliferation of hFOB osteoblasts in a concentration-dependent manner (Supplemental data Figure 1).

3.2 | Anthocyanins reduced apoptosis induced by serum starvation in hFOB cells

Serum starvation of hFOB osteoblasts (grown without FBS added to media) for 24 hr significantly reduced osteoblast proliferation (Figure 1b). However, the treatment of serum-starved hFOB osteoblasts with resveratrol (as the positive control) or ACNs at 1.0 μg/ml for an additional 72 hr increased hFOB cell proliferation as compared with serum-starved cells (Figure 1b). All four tested anthocyanins, DC, DGC, CYN, POG, and RES ($p < 0.0001$) significantly increased cell proliferation in serum-starved hFOBs (Figure 1b).

3.3 | ACNs reduce p53 and HDAC1 expression and increase Bcl-2, SIRT1, SIRT3, and PGC1α expression in apoptotic osteoblasts

Serum starvation of hFOB osteoblasts increased the expression of Bax mRNA and reduced Bcl-2 mRNA expression, significantly increased the Bax/Bcl-2 ratio ($p < 0.0001$) to favor apoptosis (Figure 2a). However, treatment of the serum-starved hFOBs with resveratrol or ACNs reduced Bax expression, increased Bcl-2 expression, and significantly reduced the Bax/Bcl-2 ratio, indicating a reduction in apoptosis (Figure 2a). Serum starvation of cultured hFOB osteoblasts also significantly increased p53 mRNA ($p < 0.0001$) and protein expression, significantly increased HDAC1 mRNA expression ($p < 0.0001$), and significantly reduced SIRT1 ($p < 0.0001$), SIRT3 ($p < 0.001$), and PGC1α mRNA expression ($p < 0.05$) (Figures 2a–f and 3) as compared with control cells in media with 10% FBS. Treatment of the serum-starved cells with ACNs, including resveratrol or peonidin-3-O-glucoside at 1.0 μg/ml for 72 hr, significantly reduced the expression of p53 mRNA ($p < 0.0001$; Figure 2b), as well as the protein levels of p53 and acetylated-p53 expression (Figure 3). Treatment of serum-starved hFOBs with ACNs also increased cell proliferation, ATP production (Supplemental data Figure 2), and RES, CYN, DGC, and POG significantly increased SIRT1 mRNA and protein expression (Figures 2e and 3), suggesting that similar to resveratrol, the ACNs activated SIRT1. Sirtuin 1 (SIRT1) is nicotinamide adenine dinucleotide (NAD+)-dependent deacetylase that has been reported to increase bone mass (Brunet et al., 2004; Buhrmann et al., 2014; Cohen-Kfir et al., 2011; Edwards et al., 2013) and shown to directly reduce the acetylation of p53 and NF-κβ, leading to a suppression of apoptosis (Brunet et al., 2004; Edwards et al., 2013). SIRT1 activation also deacetylates and increases target gene expression to increase cell proliferation and reduce oxidation and apoptosis (Brunet et al., 2004; Buhrmann et al., 2014; Edwards et

al., 2013). Thus, similar to resveratrol, these data suggest that ACNs act as SIRT1 agonists. In addition to SIRT1, resveratrol and ACNs significantly increased the expression of SIRT3 and PGC1α mRNA (Figure 2d,f) and inhibited HDAC1, suggesting that these compounds impact mitochondrial biogenesis and bone epigenome.

3.4 | ACNs increase osteoblast differentiation and *Sp7/osterix* gene expression in transgenic medaka

A zinc finger transcription factor, *Sp7* (also known as *osterix*), plays an important regulatory role in the differentiation of pre-osteoblasts to mature osteoblasts in humans, but also has a highly restricted expression in the skeletal regions of medaka (Renn & Winkler, 2009). *Sp7/osterix* is expressed in medaka in regions of early bone formation, but its expression also remains high in differentiated mature osteoblasts that mineralize the bone matrix (Renn & Winkler, 2009) (Supplemental data Figure 3). To determine if resveratrol and ACNs increase *Sp7/osterix* expression and osteoblast differentiation, *Sp7/osterix*:mCherry transgenic medaka expressing mCherry under the control of the *Sp7/osterix* promoter (Renn & Winkler, 2009; 2010) were treated at 9 dpf for 5 days with either 10 μg/ml of RES or 5 μg/ml of POG. Control fish were treated with vehicle solvent (DMSO 0.01%) only. In double transgenic *Sp7/osx*:mCherry, treatment with RES ($p < 0.0001$) and POG ($p < 0.001$) significantly increased osteoblast proliferation and gene expression of *Sp7/osx* (Figure 4a,b).

Thus, our data suggest that both RES and POG increase the proliferation and differentiation of osteoblasts by increasing *osterix/Sp7* expression.

3.5 | ACN treatments reduce RANKL-stimulated bone resorption in transgenic medaka

The efficacy of ACNs and resveratrol were assessed on RANKL-induced ectopic osteoclast formation in double transgenic medaka line *col10a1*:nlGFP/*rankl*:HSE:CFP after heat shock treatment at 9 dpf. In these medaka, heat-shock-induced RANKL expression and increased the ectopic formation of osteoclasts (Renn & Winkler, 2010; To et al., 2012). After heat shock, the medaka were immediately treated with 2.5, 5, or 10 μg/ml of resveratrol or 0.5–4 μg/ml of CYN and POG in the fish medium. The control medaka (without heat shock) show no induction of RANKL expression and continued to develop a mineralized vertebral column, along with normal centra and neural arches at 14 dpf (measured by fluorescence microscopy in Figure 5a, and by live staining with Alizarin Complexone (ALC) in Figure 5a′. In the RANKL-induced control fish (Figure 5b), there was a significant increase in mineralized matrix resorption that led to the loss of mineralized neural arches and lesions in the vertebral centra as shown in fluorescence in Figure 5b and after AR staining (Figure 5b′).

However, treatment of the medaka with resveratrol at all concentrations tested for 5 days reduced RANKL-induced osteoclastogenesis and reduced excessive bone resorption by increasing the mineralized bone matrix (shown by fluorescence microscopy in Figure 5c–e and by live ALC staining in Figure 5c′–e′). These results were also confirmed by fixed staining of the medaka vertebral column (Figure 6a–d). Resveratrol, at 10 μg/ml, reduced RANKL-induced bone resorption and protected the bone integrity of the neural arches by improving mineralization of the centra and neural arches by 88%, $p < 0.01$ (Figures 5 and

6). Similar effects were observed when heat-shocked medaka were treated with low doses (0.5–4 μg/ml) of CYN, and POG (Figures 7 and 8). For CYN (Figure 7a–d), medaka were heat shocked at 9 dpf and fixed bone staining of the mineralized vertebral column with Alizarin Red occurred after 5 days of treatment (14 dpf). The results showed heat shock of these medaka induced a loss of neural arches and degradation of the centra as compared with control (Figure 7a,b). Treatment with 0.5 μg/ml of CYN did not reduce heatshock-induced bone resorption but appeared to increase the loss of mineralization in the centra (Figure 7c). However, treatment of the medaka with 2.0 μg/ml CYN reduced mineralized bone matrix degradation by RANKL-induced ectopic osteoclasts by 21%, $p < 0.05$ (Figure 7d). Treatment of the medaka with POG also reduced mineralized matrix degradation of the centra and neural arches, and reduced bone resorption after heat-shock induction of RANKL in double transgenic (*Col10a1*:mGFP/*Rankl*:HSE:CFP) medaka larvae (Figure 8a–d). The control medaka with no RANKL induction (Figure 8a) continued the development of a mineralized vertebral column with normal centra and neural arches at 14 dpf as seen by fixed staining with Alizarin Red. However, in the heat-shocked RANKL-induced controls (Figure 8b), a significant loss in the mineralization of the neural arches and centra was observed by fixed staining at 14 dpf. Treatment with POG at 1.0 or 2.0 μg/ml for 5 days after heat shock shows a reduction in RANKL-induced mineralized bone matrix degradation by 53 and 85%, respectively, $p < 0.05$ (Figure 8c,d), suggesting a dose effect.

4 | DISCUSSION

Many animal models have been used for skeletal research under both normal and pathological conditions, including rats, mice, and chickens. However, novel vertebrate models, including teleost fish, are increasing in popularity due to their relative transparency that allows for noninvasive in vivo imaging of living specimens using highly sophisticated imaging instruments such as micro-computed tomography (μCT), confocal and fluorescence microscopy, as well as magnetic resonance imaging (MRI). Teleost fish, such as medaka (*O. latipes*), are now well-established models for use in skeletal research, and there are thousands of publications reporting the unique utility of these models. Similar to mammals, medaka fish develop bone directly from mesenchymal condensation (membranous bone formation) and on cartilage scaffolds, and bone remodeling in medaka depends on osteoclast–osteoblast interactions (Imangali et al., 2020; Renn & Winkler, 2009, 2010). In addition, bone resorption in medaka proceeds by the activation of small mononucleated osteoclasts expressing both cathepsin K (Ctsk) and tartrate-resistant acid phosphatase (TRAP) (To et al., 2012; Yu & Winkler, 2017). Furthermore, the optical clarity of the almost transparent medaka embryos and larvae permits for imaging of osteoblast proliferation, movement, and function at high resolution in live intact specimens (Renn & Winkler, 2009, 2010; To et al., 2012; Yu & Winkler, 2017), allowing for the capacity to combine powerful genetics with high-resolution imaging (Renn & Winkler, 2009, 2010). Thus, medaka are an important vertebrate model for skeletal research.

Natural products have long been used for the management of bone disorders and healing. Identified compounds, including phenolic acids, sulforaphane, resveratrol, and many others, have been shown to impact osteoblastogenesis or osteoclastogenesis, or both (An et al., 2016; Arjmandi et al., 2017; Che et al., 2016; Imangali et al., 2020; Raut et al., 2019;

Wallace, 2017). Clinical trials have shown that diets high in anthocyanins and resveratrol significantly improve bone parameters and reduce bone loss (Bo et al., 2018; Domitrovic, 2011; Ornstrup et al., 2014; Welch et al., 2012); however, the cellular and molecular mechanisms of action of ACNs have not been fully investigated. Numerous in vitro and in vivo studies have demonstrated that resveratrol increases both osteoblast differentiation and function, as well as reduces bone resorption (He et al., 2015; Imangali et al., 2020; Raut et al., 2019; Tseng et al., 2011). In addition, clinical trials have shown that treatment of obese men and in patients with type 2 diabetes 500–1,000 mg per day of resveratrol enhanced bone mineral density (Bo et al., 2018; Ornstrup et al., 2014).

In animal and cell culture studies, resveratrol has been shown to increase osteoblast proliferation and reduce bone loss by increasing the expression of BMP2, Runx2, and SIRT1, and suppressing RANKL-induced NF-kβ activation and bone loss (He et al., 2015; Mizutani et al., 1998; Su et al., 2018; Tseng et al., 2011; Zhao et al., 2018). In terms of ACNs, both delphinidin and cyanidin-3-glucoside (C3G) were reported to reduce bone resorption in rodent models; however, the mechanisms were not reported (Moriwaki et al., 2014; Park et al., 2015). In addition, fruit extracts, such as blackcurrant and acai extracts, that are high in anthocyanidin content, also have been reported to increase in vitro and in vivo osteoblast proliferation and differentiation, and the ACN compounds, delphinidin and delphinidin-O-glucoside, reduced RANKL-induced bone resorption in medaka (Eggers-Woodard et al., 2018; Huynh et al., 2017; Imangali et al., 2020; Mahady, Raut, et al., 2019; Mahady, Raut, & Lawal, 2019; Raut et al., 2018, 2019). However, the effects of ACNs on osteoblast differentiation and gene expression, as well as RANKL-induced bone resorption in *Sp7/osx*:mCherry and *col10a1*:mGFP/*rankl*:HSE:CFP medaka, have not been previously reported.

In this work, we demonstrate that resveratrol and peonidin-3-O-glucoside both significantly ($p < 0.0001$; $p < 0.001$, respectively) increased the proliferation of human hFOB 1.19 osteoblasts in vitro, while cyanidin, delphinidin, and delphinidin-O-glucoside were not active. However, induction of apoptosis in human osteoblasts by serum starvation was significantly reduced by resveratrol and all ACNs tested at 1 μg/ml ($p < 0.0001$). Serum-starved (SS) osteoblasts showed significant ($p < 0.0001$) increase in the Bax/Bcl2 ratio as compared with control osteoblasts grown in 10% FBS, indicating induction of apoptosis. When SS-osteoblasts were treated with resveratrol, delphinidin, delphinidin-O-glucoside, cyanidin, and peonidin-3-O-glucoside for 72 hr, there was significant reduction in the Bax/Bcl2 ratio ($p < 0.0001$), and an increase in cell proliferation. Serum starvation of osteoblasts also significantly increased the expression of HDAC1 mRNA ($p < 0.0001$) and p53 mRNA and protein ($p < 0.0001$), and reduced SIRT1 mRNA and protein ($p < 0.0001$) expression. Treatment of the SS-hFOB osteoblasts with resveratrol and ACNs reversed this pattern, and significantly downregulated both HDAC1 ($p < 0.0001$) and p53 expression ($p < 0.0001$), and upregulated Bcl-2, SIRT1 ($p < 0.05$–0.0001) and SIRT3 ($p < 0.05$–0.0001) expression and reduced Bax mRNA expression. These results suggest that similar to resveratrol, ACNs reduce osteoblast apoptosis through epigenetic mechanisms involving SIRT1, SIRT3, and HDAC1. These data correlate well with those published by He et al. (2015), who reported that resveratrol inhibited apoptosis in cultured mouse osteoblast MC3T3-E1 induced by hydrogen peroxide by activating SIRT1 and Bcl-2 expression, and decreasing Bax and p53

expression. Furthermore, Zhao et al. (2018) reported that treatment of mice with resveratrol enhanced osteoblast activity and bone mineralization, by activating both SIRT1 and BMP2. Thus, our data suggest that the effects of ACNs on human osteoblasts are similar to resveratrol, and proceed via the activation of SIRT1 and 3, and by inhibition of HDAC1 and p53 expression. Park et al. (2015) have reported that cyanidin-3-glucoside also stimulated formation of bone by increasing in vitro differentiation and proliferation of osteoblasts; however, the mechanisms of action were not reported (Park et al., 2015).

Sirtuins (silent information regulator 2 [Sir2] family) are NAD +-dependent protein deacetylases, whose activation reduces the activation of cellular reactive oxygen species (ROS) and suppresses apoptosis (Hori et al., 2013; Horio et al., 2012; Huynh et al., 2017; Raut et al., 2019). SIRT1 activation has been shown to alter important transcription factors that impact cell survival and apoptosis, such as p53, a tumor suppressor protein, and is a regulator of mitochondrial biogenesis, and PGC1α (Luo et al., 2001; Vaziri et al., 2001; Vousden, 2000). An increase in reactive oxygen species (ROS) concentrations induces DNA damage, thereby increasing the expression of pro-apoptotic proteins such as Bax and p53, which eventually target the mitochondria and induce apoptosis (Vousden, 2000). SIRT1 agonists increase the deacetylation of p53, thereby reducing its apoptotic activity (Horio et al., 2012; Luo et al., 2001; Vaziri et al., 2001; Vousden, 2000). Our data suggest that specific ACNs act as SIRT1 agonists and reduce p53 mRNA and protein expression, as well as acetylated p53 protein expression. In terms of osteoblastogenesis, it has been suggested that p53 may impact bone remodeling by altering the expression of transcription factor, *Sp7/osx*, thereby increasing or decreasing osteoblast differentiation (Achanta & Huang, 2004; Artigas et al., 2017; Wang et al., 2006). Both in vitro and in vivo investigations have shown that *Sp7/osx* expression is increased in the absence of p53, and *Sp7/osx* expression and osteoblast differentiation were reduced when p53 expression was upregulated (Wang et al., 2006). Artigas et al. (2017), have further demonstrated that p53 inhibited *Sp7/osx* transcriptional activity, and hypothesized that p53 is a novel regulator of osteoblast differentiation and bone remodeling.

In this work, we show that resveratrol and ACNs in low concentrations reduced osteoblast apoptosis, and this effect was correlated with decreased p53 gene and protein expression and an increased SIRT1/3 expression. Furthermore, transgenic medaka treated with low concentrations of resveratrol and peonidin-3-O-glucoside exhibited increased *Sp7/osx* expression, indicating osteoblast differentiation. Artigas et al. (2017) reported that *Sp7/osx* regulates osteoblast differentiation and the transcription of osteoblast-related genes by indirectly binding to the homeobox transcription factor Dlx. Our data show that ACNs, like resveratrol, act as SIRT1 agonists and p53 antagonists to increase osteoblast differentiation and activate *Sp7/osx*.

Activation of SIRT1 is transcriptional and associated with an increase in mitochondrial metabolism and antioxidant effects and has also been reported to impact other SIRTs, including SIRT3 (Hori et al., 2013; Horio et al., 2012; Huynh et al., 2017). SIRT3 is present in the mitochondria and impacts mitochondrial function by deacetylating and regulating the activity of proteins involved in intermediary metabolism, fatty acid oxidation, and oxidative stress responses (Hori et al., 2013; Horio et al., 2012). SIRT1 deacetylates and increases

expression of PGC1α that is associated with an increase in SIRT3 gene expression, so SIRT1 appears to increase the transcription of SIRT3 (Hori et al., 2013; Horio et al., 2012; Huynh et al., 2017). Gao et al. (2018) found that the mitochondrial redox and function played a critical role in osteoblast differentiation and bone formation, and that this role was controlled by SIRT3/SOD2. Interestingly, Roos et al. (2017) found that the expression of *Runx2* and *Sp7/osterix* were decreased in SIRT3 deficient mice, indicating that SIRT3 is necessary for osteoblast differentiation (Roos et al., 2017). Thus, our data show that, along with increased SIRT1 expression, ACNs significantly increased the production of ATP and the expression of both PGC1α and SIRT3, suggesting that these compounds may also increase osteoblast differentiation by increasing mitochondrial activity.

In addition to SIRTs, we have also observed that specific ACNs inhibited the expression of HDAC1, of which peonidin-3-O-glucoside was also the most active. A number of studies have shown that histone deacetylase inhibitors (HDACi) promote osteoblast differentiation both in vitro and ex vivo (Bradley et al., 2011; Huynh et al., 2017; Raut et al., 2019). In addition to their effects on histone proteins, HDACs also deacetylate non-histone proteins, including transcription factors that are involved in the formation of bone (Huynh et al., 2017; Raut et al., 2019; Roos et al., 2017). HDACs have been shown to regulate both chondrocyte and osteoblast differentiation and activities through interactions with transcription factors including Runx2, Smads, Twist, and PRb and inhibit the activity of Runx2, thereby suppressing osteoblast differentiation (Bradley et al., 2011; Huynh et al., 2017). HDACIs, however, have been shown to accelerate osteoblast differentiation (Bradley et al., 2011; Huynh et al., 2017). We have previously reported that ACNs increased *Runx2* and *Sp7/osx* expression in cultured osteoblasts (Mahady, Raut, & Lawal, 2019; Raut et al., 2019), and, in this work, the data show that the ACNs also reduced HDAC1 expression, suggesting that some of these compounds may act as HDACIs, to increase *Runx2* expression and promote osteoblast differentiation.

In terms of bone resorption, heat shock-induced RANKL expression our double transgenic *col10a1*:nlGFP/*rankl*:HSE:CFP medaka induced the formation of ectopic osteoclasts, thereby reducing bone mineralization and the notochordal sheath. Control medaka (without RANKL induction) continued the development of a mineralized vertebral column with normal centra and neural arches at 14 dpf. However, heat-shocked medaka exhibited activated osteoclasts and increased the resorption of the mineralized bone matrix, causing 100% loss of the neural arches and significant degradation of the centra. Heat-shocked medaka were treated with 2.5, 5, or 10 μg/ml of resveratrol or 0.5–4 μg/ml of ACNs in the medium for 5 days, starting from the day of RANKL induction, the integrity of neural arches was protected by 21–88% depending on the compound and dose tested, and there was a reduction in centra degradation. These data suggest that similar to resveratrol, ACNs reduced the formation of ectopic osteoclasts, thereby reversing bone resorption and increasing bone mineralization. Resveratrol, cyanidin, and peonidin-3-O-glucoside reduced RANKL-induced bone resorption in a dose-dependent manner; however, both cyanidin and peonidin-3-O-glucoside were effective in lower doses (1–2 μg/ml peonidin-3-O-glucoside versus 10 μg/ml of resveratrol). Previous studies have shown that both cyanidin-3-O-glucoside and delphinidin reduced osteoclastogenesis after RANKL induction in vitro (Imangali et al., 2020; Mahady, Nishikant, & Lawal, 2019). We have previously reported that bone resorption

in a medaka model of osteoporosis has been prevented by treatment with DC and DGC, inhibiting differentiation of osteoclasts induced by RANKL (Imangali et al., 2020). Park et al. (2015) also reported that cyanidin-3-O-glucoside, dose-dependently, reduced RANKL-mediated osteoclast differentiation and formation, and reduced the activities of extracellular signal-regulated kinase, c-Jun N-terminal kinase, and p38 mitogen-activated kinases. This group also reported that cyanidin-3-O-glucoside also increased osteoblast differentiation and matrix formation (Park et al., 2015), further supporting our findings.

5 | CONCLUSION

Similar to resveratrol, specific ACNs increased osteoblast differentiation and reduced RANKL-induced ectopic osteoclast formation. In transgenic medaka, the ACNs were more active than resveratrol in that they were effective at 5–10-fold lower doses. This work further suggests that ACNs likely have multiple mechanisms of action, in that they inhibited HDAC1 in cultured human hFOB osteoblasts, increased SIRT1/3 and PGC1α expression, and acted as p53 antagonists. In *Sp7/osx*:mCherry transgenic medaka, both peonidin-3-O-glucoside and resveratrol increased *Sp7/osx* and *Runx2* expression along with osteoblast proliferation and differentiation. In transgenic *Col10a1*:mGFP/*Rankl*:HSE:CFP medaka, cyanidin, peonidin-3-O-glucoside, and resveratrol reduced RANKL-induced bone resorption, of which peonidin-3-glucoside was the most active compound, with an effective dose of 2 μg/ml. Thus, since cyanidin and peonidin-3-O-glucoside both increased osteoblast differentiation and reduced RANKL-induced bone resorption, and they could be developed as a novel therapies for osteoporosis. Transcriptomic studies are underway to develop a more comprehensive understanding of the biological pathways involved in the effects of these compounds on the bone genome and epigenome.

Supplementary Material

Refer to Web version on PubMed Central for supplementary material.

ACKNOWLEDGEMENT

This research was funded in part by a grant from the National Center for Complementary and Integrative Health at the National Institutes of Health (NIH; R21 AT008452) to GBM; a Schlumberger Foundation Fellowship award to TOL; and a Raman Post-Doctoral Fellowship by University Grants Commission, Govt. of India [F.No.5–66/2016 (IC) Dtd. Feb. 10, 2016] to NAR. The contents are solely the responsibility of the authors and do not necessarily represent the official views of the NCCIH or NIH, or the other funding agencies.

Funding information

National Center for Complementary and Integrative Health at the National Institutes of Health, Grant/Award Number: NIH; R21 AT008452 to GBM; University Grants Commission, Grant/Award Number: Raman Fellowship, F.No.5–66/2016(IC) Dtd. Feb. 10, 2016; Schlumberger Foundation; National Institutes of Health; National Center for Complementary and Integrative Health

REFERENCES

Achanta G, & Huang P. (2004). Role of p53 in sensing oxidative DNA damage in response to reactive oxygen species-generating agents. Cancer Research, 64(17), 6233–6239. https://cancerres.aacrjournals.org/content/64/17/6233.short [PubMed: 15342409]

An J, Yang H, Zhang Q, Liu C, Zhao J, Zhang L, & Chen B. (2016). Natural products for treatment of osteoporosis: The effects and mechanisms on promoting osteoblast-mediated bone formation. Life Sciences, 147, 46–58. 10.1016/j.lfs.2016.01.024 [PubMed: 26796578]

Appelman-Dijkstra NM, & Papapoulos SE (2018). Paget's disease of bone. Best Practice & Research. Clinical Endocrinology & Metabolism, 32, 657–668. [PubMed: 30449547]

Arjmandi BH, Johnson SA, Pourafshar S, Navaei N, George KS, Hooshmand S, … Akhavan NS (2017). Bone-protective effects of dried plum in postmenopausal women: Efficacy and possible mechanisms. Nutrients, 9, 496. 10.3390/nu9050496

Artigas N, Gámez B, Cubillos-Rojas M, Sánchez-De Diego C, Valer JA, Pons G, … Ventura F. (2017). P53 inhibits SP7/Osterix activity in the transcriptional program of osteoblast differentiation. Cell Death and Differentiation, 24(12), 2022–2031. 10.1038/cdd.2017.113 [PubMed: 28777372]

Bo S, Gambino R, Ponzo V, Cioffi I, Goitre I, Evangelista A, … Procopio M. (2018). Effects of resveratrol on bone health in type 2 diabetic patients. A double-blind randomized-controlled trial. Nutrition and Diabetes, 8(51), 1–10. 10.1038/s41387-018-0059-4 [PubMed: 29330446]

Bradley EW, McGee-Lawrence ME, & Westendorf JJ (2011). Hdac-mediated control of endochondral and intramembranous ossification. Critical Reviews™ in Eukaryotic Gene Expression, 21(2), 101–113. 10.1615/critreveukargeneexpr.v21.i2.10

Brunet A, Sweeney LB, Sturgill JF, Chua KF, Greer PL, Lin Y, … Greenberg ME (2004). Stress-dependent regulation of FOXO transcription factors by the SIRT1 deacetylase. Science, 303(5666), 2011–2015. 10.1126/science.1094637 [PubMed: 14976264]

Buhrmann C, Busch F, Shayan P, & Shakibaei M. (2014). Sirtuin-1 (SIRT1) is required for promoting chondrogenic differentiation of mesenchymal stem cells. ASBMB, 289(32), 22048–22062. 10.1074/jbc.M114.568790

Chang G, Boone S, Martel D, Rajapakse CS, Hallyburton RS, Valko M, … Regatte RR (2017). MRI assessment of bone structure and microarchitecture. Journal of Magnetic Resonance Imaging, 46(2), 323–337. 10.1002/jmri.25647 [PubMed: 28165650]

Che CT, Wong MS, Lam CWK, & McPhee DJ (2016). Natural products from Chinese medicines with potential benefits to bone health. Molecules, 21(239), 1–52. 10.3390/molecules21030239

Chen X, Sun K, Jiao S, Cai N, Zhao X, Zou H, … Wei L. (2014). High levels of SIRT1 expression enhance tumorigenesis and associate with a poor prognosis of colorectal carcinoma patients. Scientific Reports, 4(7481), 1–12. 10.1038/srep07481

Cheng J, Zhou L, Liu Q, Tickner J, Tan Z, Li X, … Xu J. (2018). Cyanidin chloride inhibits ovariectomy-induced osteoporosis by suppressing RANKL-mediated osteoclastogenesis and associated signaling pathways. Journal of Cellular Physiology, 233(3), 2502–2512. 10.1002/jcp.26126 [PubMed: 28771720]

Cohen-Kfir E, Artsi H, Levin A, Abramowitz E, Bajayo A, Gurt I, … Dresner-Pollak R. (2011). Sirt1 is a regulator of bone mass and a repressor of sost encoding for sclerostin, a bone formation inhibitor. Endocrinology, 152(12), 4514–4524. 10.1210/en.2011-1128 [PubMed: 21952235]

Danks L, Komatsu N, Guerrini MM, Sawa S, Armaka M, Kollias G, … Takayanagi H. (2016). RANKL expressed on synovial fibroblasts is primarily responsible for bone erosions during joint inflammation. Annals of the Rheumatic Diseases, 75(6), 1187–1195. 10.1136/annrheumdis-2014-207137 [PubMed: 26025971]

Domitrovic R. (2011). The molecular basis for the pharmacological activity of anthocyans. Current Medicinal Chemistry, 18(29), 4454–4469. 10.2174/092986711797287601 [PubMed: 21864288]

Edwards JR, Perrien DS, Fleming N, Nyman JS, Ono K, Connelly L, … Elefteriou F. (2013). Silent information regulator (Sir) T1 inhibits NF-κB signaling to maintain normal skeletal remodeling. Journal of Bone and Mineral Research, 28(4), 960–969. 10.1002/jbmr.1824 [PubMed: 23172686]

Eggers-Woodard NA, Wicks SM, Raut N, Yu TS, Winkler C, Mahady GB, & Carcache de Blanco EJ (2018). Acai exhibits antidiabetic and osteogenic activities in fish models. American Society of Pharmacognosy Annual Meeting, July 21–25, 2018.

Feng X, & McDonald JM (2011). Disorders of bone remodeling. Annual Review of Pathology, 6, 121–145.

Gao J, Feng Z, Wang X, Zeng M, Liu J, Han S, … Liu J. (2018). SIRT3/SOD2 maintains osteoblast differentiation and bone formation by regulating mitochondrial stress. Cell Death and Differentiation, 25(2), 229–240. 10.1038/cdd.2017.144 [PubMed: 28914882]

Haas AV, & LeBoff MS (2018). Osteoanabolic agents for osteoporosis. Journal of the Endocrine Society, 2(8), 922–932. 10.1210/js.2018-00118 [PubMed: 30087947]

He N, Zhu X, He W, Zhao S, Zhao W, & Zhu C. (2015). Resveratrol inhibits the hydrogen dioxide-induced apoptosis via Sirt 1 activation in osteoblast cells. Bioscience, Biotechnology and Biochemistry, 79(11), 1779–1786. 10.1080/09168451.2015.1062712

Hori Y, Kuno A, Hosoda R, & One YH (2013). Regulation of FOXOs and p53 by SIRT1 modulators under oxidative stress. PLoS One, 8(9), e73875. https://www.ncbi.nlm.nih.gov/pmc/articles/PMC3770600/

Horio Y, Hayashi T, Kuno A, & Science RK (2012). Cellular and molecular effects of sirtuins in health and disease. Journal of Cellular Biochemistry, 113, 752–759. 10.1002/jcb.23431 [PubMed: 22065601]

Hou D-X, Ose T, Lin S, Harazoro K, Imamura I, Kubo M, … Fujii M. (2003). Anthocyanidins induce apoptosis in human promyelocytic leukemia cells: Structure-activity relationship and mechanisms involved. International Journal of Oncology, 23(3), 705–712. 10.3892/ijo.23.3.705 [PubMed: 12888907]

Huynh NCN, Everts V, & Ampornaramveth RS (2017). Histone deacetylases and their roles in mineralized tissue regeneration. Bone Reports, 7, 33–40. 10.1016/j.bonr.2017.08.001 [PubMed: 28856178]

Imangali N, Phan QT, Mahady G, & Winkler C. (2020). The dietary anthocyanin delphinidin prevents bone resorption by inhibiting Rankl-induced differentiation of osteoclasts in a medaka (Oryzias latipes) model of osteoporosis. Journal of Fish Biology, Special Issue, 98, 1018–1030. 10.1111/jfb.14317 [PubMed: 32155282]

IOF. (2017). Epidemiology. Osteoporosis & Musculoskeletal Disorders Published by International Osteoporosis Foundation. https://www.iofbonehealth.org/epidemiology

Jayaprakasam B, Vareed SK, Olson LK, & Nair MG (2005). Insulin secretion by bioactive anthocyanins and anthocyanidins present in fruits. Journal of Agricultural and Food Chemistry, 53(1), 28–31. 10.1021/jf049018+ [PubMed: 15631504]

Kanis JA, McCloskey EV, Johansson H, Cooper C, Rizzoli R, & Reginster JY (2013). European guidance for the diagnosis and management of osteoporosis in postmenopausal women. Osteoporosis International, 24(1), 23–57. 10.1007/s00198-012-2074-y [PubMed: 23079689]

Lee SG, Kim B, & Vance TM (2014). Relationship between oxidative stress and bone mass in obesity and effects of berry supplementation on bone remodeling in obese male mice: An exploratory study development of analytical technique to authenticate sesame oil view project HDL metabolism view. Article in Journal of Medicinal Food, 18(4), 476–482. 10.1089/jmf.2013.0182 [PubMed: 25198411]

Lee SG, Vance TM, Nam TG, Kim DO, Koo SI, & Chun OK (2015). Contribution of anthocyanin composition to total antioxidant capacity of berries. Plant Foods for Human Nutrition, 70(4), 427–432. 10.1007/s11130-015-0514-5 [PubMed: 26515081]

Liu Y, & Bodmer WF (2006). Analysis of P53 mutations and their expression in 56 colorectal cancer cell lines. Proceedings of the National Academy of Sciences of the United States of America, 103(4), 976–981. 10.1073/pnas.0510146103 [PubMed: 16418264]

Luo J, Nikolaev AY, Imai S, Chen D, Su F, Shiloh A, … Gu W. (2001). Negative control of p53 by Sir2α promotes cell survival under stress. Cell, 107(2), 137–148. 10.1016/S0092-867400524-4 [PubMed: 11672522]

Mahady G, Raut N, Lawal T, & Patel S. (2019). Epigenetic regulation of osteoblastogenesis by blackcurrant fruit extracts in vitro and in vivo. FASEB Journal, 33(1), 471.14. 10.1096/fasebj.2019.33.1_supplement.471.14

Mahady GB, Raut N, & Lawal TO (2019). Acai fruit extracts and anthocyanins alter osteoblast proliferation and the expression of HDAC1 and osterix/Sp7 in vitro and in vivo. FASEB Journal, 33(1), 515.14. 10.1096/fasebj.2019.33.1_supplement.515.14

Manolagas SC (2010). From estrogen-centric to aging and oxidative stress: A revised perspective of the pathogenesis of osteoporosis. Endocrine Reviews, 31(3), 266–300. 10.1210/er.2009-0024 [PubMed: 20051526]

McGowen JA, Raisz LG, Noonan AS, Elderkin AL (2004). Bone health and osteoporosis: A report of the Surgeon General. https://www.iofbonehealth.org/sites/default/files/PDFs/2004_us_surgeon_generals_report.pdf

Mizutani K, Ikeda K, Kawai Y, & Yamori Y. (1998). Resveratrol stimulates the proliferation and differentiation of osteoblastic MC3T3-E1 cells. Biochemical and Biophysical Research Communications, 253(3), 859–863. 10.1006/bbrc.1998.9870 [PubMed: 9918820]

Moriwaki S, Suzuki K, Muramatsu M, Nomura A, & Inoue F. (2014). Delphinidin, one of the major Anthocyanidins, prevents bone loss through the inhibition of excessive osteoclastogenesis in osteoporosis model mice. PLoS One, 9(5), 97177. 10.1371/journal.pone.0097177

Mulabagal V, Keller WJ, & Calderon AI (2012). Quantitative analysisof anthocyanins in Euterpe oleracea (açaí) dietary supplement raw materials and capsules by Q-TOF liquid chromatography/mass spectrometry. Pharmaceutical Biology, 50(10), 1289–1296. 10.3109/13880209.2012.674141 [PubMed: 22900515]

Ornstrup MJ, Harsløf T, Kjær TN, Langdahl BL, & Pedersen SB (2014). Resveratrol increases bone mineral density and bone alkaline phosphatase in obese men: A randomized placebo-controlled trial. Journal of Clinical Endocrinology and Metabolism, 99(12), 4720–4729. 10.1210/jc.2014-2799 [PubMed: 25322274]

Ouaïssi M, Silvy F, Loncle C, Da Silva DF, Abreu CM, Martinez E, … Mas E. (2014). Further characterization of HDAC and SIRT gene expression patterns in pancreatic cancer and their relation to disease outcome. PLoS One, 9(10), e108520. 10.1371/journal.pone.0108520

Park KH, Gu DR, So HS, Kim K, & Lee SH (2015). Dual role of cyanidin-3-glucoside on the differentiation of bone cells. Article in Journal of Dental Research, 94(12), 1676–1683. 10.1177/0022034515604620 [PubMed: 26350961]

Qaseem A, Forciea MA, McLean RM, & Denberg TD (2017). Treatment of low bone density or osteoporosis to prevent fractures in men and women: A clinical practice guideline update from the American college of physicians. Annals of Internal Medicine, 166(11), 818–839. 10.7326/M15-1361 [PubMed: 28492856]

Raut N, Wicks SM, Lawal TO, & Mahady GB (2019). Epigenetic regulation of bone remodeling by natural compounds. Pharmacological Research, 147, 104350. 10.1016/j.phrs.2019.104350

Raut N, Wicks SM, Yu TS, Winkler C, Ren Z, Lee SM, & Mahady GB (2018). Osteogenic effects of blackcurrant and acai extracts in human hFOB osteoblasts and transgenic medaka. 24th International Conference of the Functional Foods Center - 12th International Symposium of ASFFBC, Functional Foods and Chronic Diseases: Science and Practice, September 20–21, 2018, Harvard Medical School, Boston, MA, USA.

Renn J, & Winkler C. (2010). Characterization of collagen type 10a1 and osteocalcin in early and mature osteoblasts during skeleton formation in medaka. Journal of Applied Ichthyology, 26(2), 196–201. 10.1111/j.1439-0426.2010.01404.x

Renn J, & Winkler C. (2009). Osterix-mCherry transgenic medaka for in vivo imaging of bone formation. Developmental Dynamics, 238(1), 241–248. 10.1002/dvdy.21836 [PubMed: 19097055]

Roos CM, Hagler MA, Verzosa GC, Zhang B, Fujimoto H, & Miller JD (2017). Abstract 427: Histopathological and Molecular Effects of SIRT3 Deletion in Advanced Calcific Aortic Valve Disease. Arteriosclerosis, Thrombosis, and Vascular Biology, 37(suppl_1). 10.1161/atvb.37.suppl_1.427

Rossini M, Adami S, Bertoldo F, Diacinti D, Gatti D, Giannini S, … Isaia GC (2016). Guidelines for the diagnosis, prevention and management of osteoporosis. Reumatismo, 68(1), 1–39. http://www.reumatismo.org/index.php/reuma/article/download/870/710 [PubMed: 27339372]

Sakaki J, Melough M, Lee SG, Kalinowski J, Koo SI, Lee SK, & Chun OK (2018). Blackcurrant supplementation improves trabecular bone mass in young but not aged mice. Nutrients, 10, 1671. 10.3390/nu10111671

Scarpulla RC (2011). Metabolic control of mitochondrial biogenesis through the PGC-1 family regulatory network. Biochimica et Biophysica Acta - Molecular Cell Research, 1813(7), 1269–1278. 10.1016/j.bbamcr.2010.09.019

Solomon H, Dinowitz N, Pateras IS, Cooks T, Shetzer Y, Molchadsky A, … Rotter V. (2018). Mutant p53 gain of function underlies high expression levels of colorectal cancer stem cells markers. Oncogene, 37(12), 1669–1684. 10.1038/s41388-017-0060-8 [PubMed: 29343849]

Sozen T, Ozisik L,& Basaran N. (2017). An overview and management of osteoporosis. European Journal of Rheumatology, 4, 46–57. [PubMed: 28293453]

Su P, Tian Y, Yang C, Ma X, Wang X, Pei J, & Qian A. (2018). Mesenchymal stem cell migration during bone formation and bone diseases therapy. International Journal of Molecular Sciences, 19(8), 2343. 10.3390/ijms19082343

To TT, Eckhard Witten P, Renn J, Bhattacharya D, Huysseune A, & Winkler C. (2012). Rankl-induced osteoclastogenesis leads to loss of mineralization in a medaka osteoporosis model. Development, 139(1), 141–150. 10.1242/dev.071035 [PubMed: 22096076]

Tseng PC, Hou SM, Chen RJ, Peng HW, Hsieh CF, Kuo ML, & Yen ML (2011). Resveratrol promotes osteogenesis of human mesenchymal stem cells by upregulating RUNX2 gene expression via the SIRT1/FOXO3A axis. Journal of Bone and Mineral Research, 26(10), 2552–2563. 10.1002/jbmr.460 [PubMed: 21713995]

Vaziri H, Dessain SK, Eaton EN, Imai SI, Frye RA, Pandita TK, … Weinberg RA (2001). hSIR2SIRT1 functions as an NAD-dependent p53 deacetylase. Cell, 107(2), 149–159. 10.1016/S0092-8674(01)00527-X [PubMed: 11672523]

Vousden KH (2000). p53: Death star. Cell, 103(5), 691–694. 10.1016/S0092-8674(00)00171-9 [PubMed: 11114324]

Wallace TC (2017). Dried plums, prunes and bone health: A comprehensive review. Nutrients, 9, 401. 10.3390/nu9040401

Wang X, Kua HY, Hu Y, Guo K, Zeng Q, Wu Q, … Li B. (2006). p53 functions as a negative regulator of osteoblastogenesis, osteoblast-dependent osteoclastogenesis, and bone remodeling. Journal of Cell Biology, 172(1), 115–125. 10.1083/jcb.200507106

Welch A, MacGregor A, Jennings A, Fairweather-Tait S, Spector T, & Cassidy A. (2012). Habitual flavonoid intakes are positively associated with bone mineral density in women. Journal of Bone and Mineral Research, 27(9), 1872–1878. 10.1002/jbmr.1649 [PubMed: 22549983]

Yu T, & Winkler C. (2017). Drug treatment and in vivo imaging of osteoblast-osteoclast interactions in a medaka fish osteoporosis model. Journal of Visualized Experiments, 2017(119), 1. 10.3791/55025

Zhao M, Ko SY, Garrett IR, Mundy GR, Gutierrez GE, & Edwards JR (2018). The polyphenol resveratrol promotes skeletal growth in mice through a sirtuin 1-bone morphogenic protein 2 longevity axis. British Journal of Pharmacology, 175(21), 4183–4192. 10.1111/bph.14477 [PubMed: 30125963]

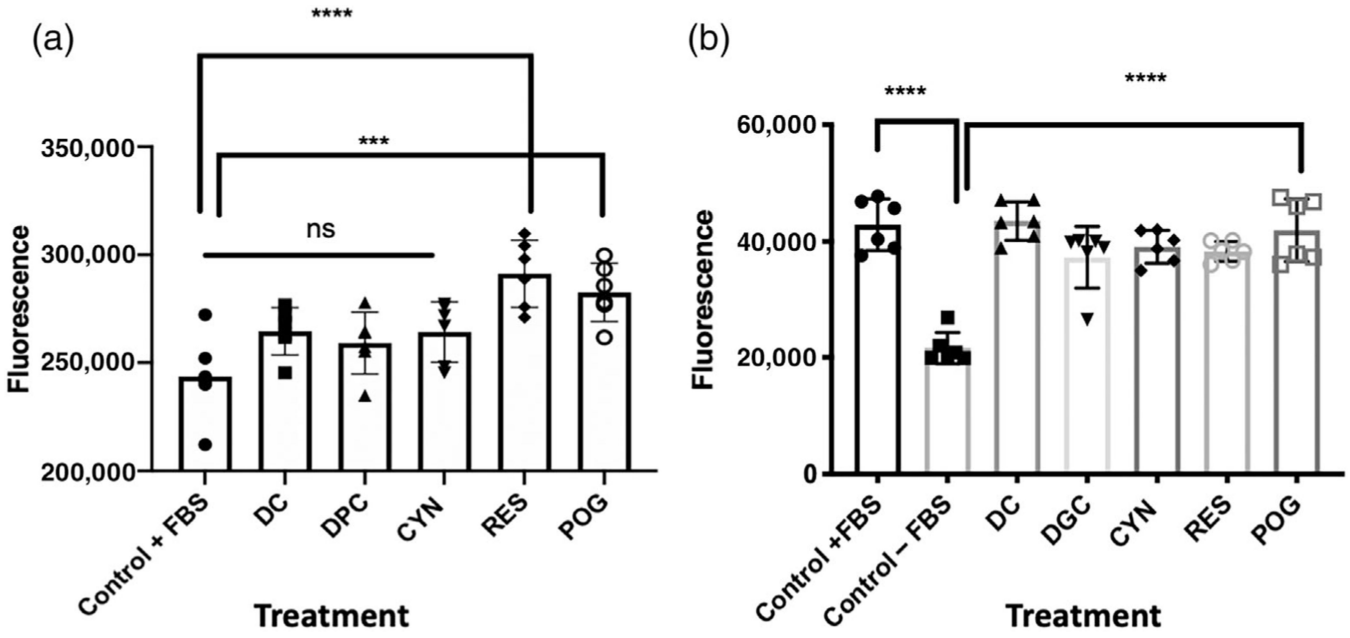

FIGURE 1.

Treatment of cultured human hFOB osteoblasts with resveratrol and anthocyanins. (a) hFOB cells were grown in media containing 10% FBS and then treated with anthocyanins for 72 hr. Control cells were treated with 0.01% DMSO. Cells were treated with delphinidin (DC); delphinidin-O-glucoside (DGC); cyanidin (CYN); resveratrol (RES); peonidin-3-O-glucoside (POG) in a concentration of 1.0 μg/ml. Control vs. DC, DGC, CYN was not significant (ns), while treatments with RES or POG significantly increased cell proliferation (***$p < 0.001$; ****$p < 0.0001$). (b) hFOB osteoblasts were serum-starved for 24 hr and then treated with anthocyanins for 72 hr. As compared with osteoblasts grown in media with 10% FBS, serum-starved (−FBS) cells showed a significant ($p < 0.0001$) reduction in growth. However, treatment of serum-starved cells with DC, DGC, CYN, RES, or POG increased cell proliferation and reduced apoptosis at a concentration of 1.0 μg/ml. Control + FBS vs. Control – FBS (****$p < 0.0001$); Control −FBS vs. DC, DGC, CYN, RES, POG (****$p < 0.0001$). Cell viability and proliferation were measured using CellTitreGLo® (Promega). Statistics were performed using one-way ANOVA followed by Dunnett's multiple comparison test using GraphPad 8.2 (San Diego, CA)

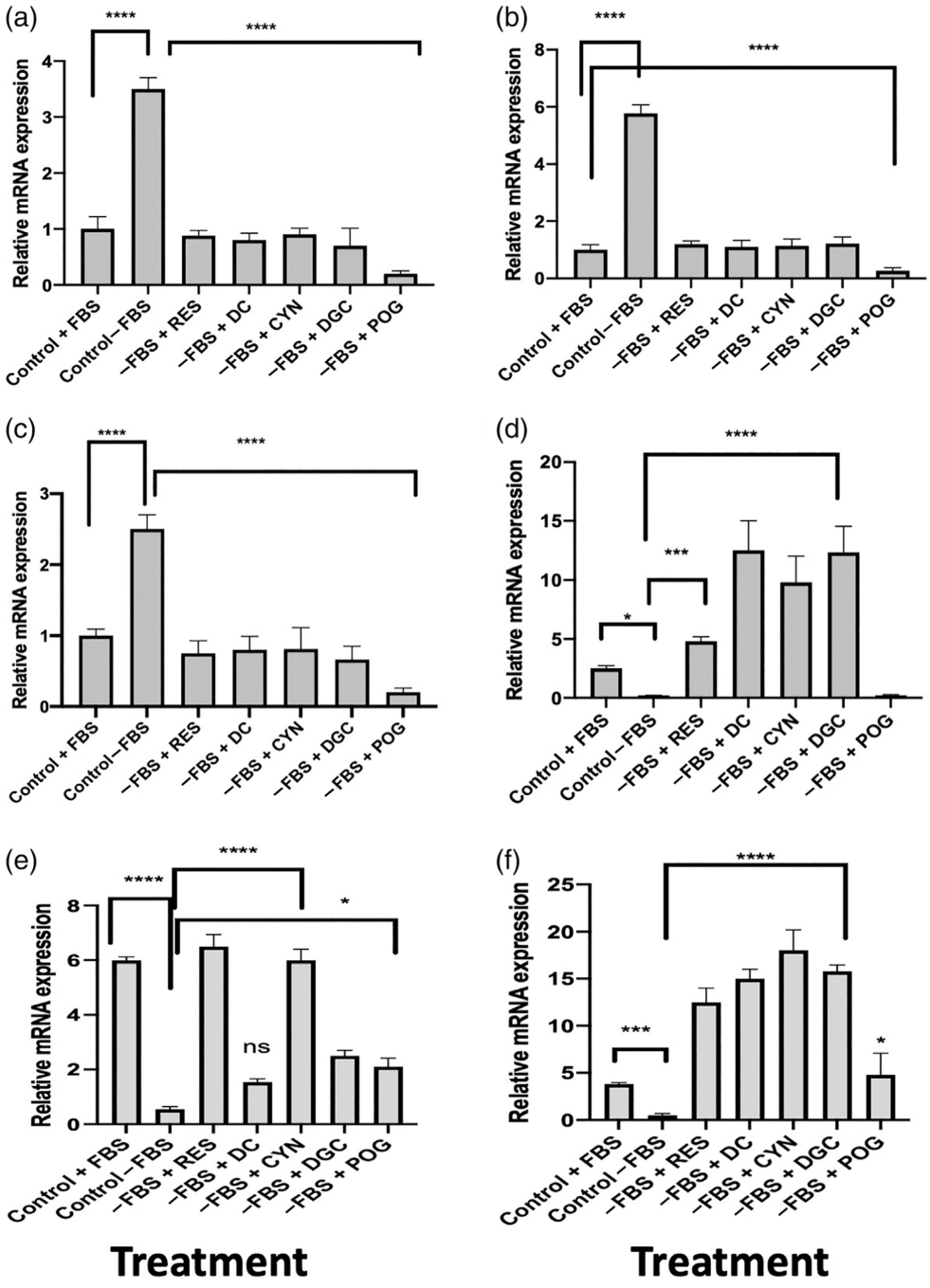

FIGURE 2.

Gene expression in hFOB human osteoblasts after treatment with resveratrol or anthocyanins. (a) The Bax/Bcl-2 ratio in hFOB osteoblasts treated with anthocyanins after serum starvation for 24 hr. Serum starvation (−FBS) significantly increased the Bax/Bcl-2 ratio as compared with normal controls (+FBS) indicating apoptosis. Treatment of the serum-starved cells with delphinidin (DC); delphinidin-O-glucoside (DGC); cyanidin (CYN); resveratrol (RES); peonidin-3-O-glucoside (POG) at 1.0 μg/ml for 72 hr reduced the Bax/Bcl-2 ratio and increased cell proliferation, suggesting a reduction in apoptosis. All

compounds significantly (****$p < 0.0001$) reduced the Bax/Bcl-2 ratio. (b) Expression of p53 mRNA in hFOB osteoblasts treated with resveratrol or ACNs after serum starvation for 24 hr. Serum starvation (−FBS) significantly increased the expression of p53 as compared with normal controls (+FBS) and induced apoptosis. Treatment of the serum-starved osteoblasts with ACNs (1.0 μg/ml) reduced p53 expression and increased cell proliferation. All compounds significantly (****$p < 0.0001$) downregulated p53 gene expression. (c) Expression of HDAC1 mRNA in hFOB osteoblasts treated with RES or ACNs after serum starvation for 24 hr. Serum starvation (−FBS) significantly increased the expression of HDAC1 as compared with normal controls (+FBS) and induced apoptosis. Treatment of the serum-starved osteoblasts with ACNs (1.0 μg/ml) reduced HDAC1 mRNA expression and increased cell proliferation. All compounds significantly (****$p < 0.0001$) downregulated HDAC1 mRNA expression. (d) Expression of PGC1α mRNA in hFOB osteoblasts treated with resveratrol or ACNs after serum starvation for 24 hr. Serum starvation (−FBS) significantly increased the expression of PGC1α as compared with normal controls (+FBS) and induced apoptosis. Treatment of the serum-starved osteoblasts with ACNs (1.0 μg/ml) reduced PGC1α mRNA expression and increased cell proliferation. All compounds significantly upregulated PGC1α expression. *$p < 0.05$; ***$p < 0.001$; ****$p < 0.0001$. (e) Expression of SIRT1 mRNA in hFOB osteoblasts treated with ACNs after serum starvation for 24 hr. Serum starvation (Control-FBS) of hFOB human osteoblasts reduced the expression of SIRT1 mRNA as compared with cells treated with 10% FBS (****$p < 0.001$). Treatment of serum-starved cells with ACNs at 1.0 μg/ml significantly increased SIRT1 expression as compared with control-FBS. Only DC treatment was not significant. *$p < 0.05$; ****$p < 0.0001$. (f) Serum starvation (control-FBS) of hFOB human osteoblasts reduced the expression of SIRT3 mRNA as compared with cells grown in 10% FBS, while treatment of serum-starved cells with ACNs at 1.0 μg/ml significantly increased SIRT3 expression as compared with control-FBS. *$p < 0.05$; ****$p < 0.0001$. Statistics were performed using one-way ANOVA followed by Dunnett's multiple comparison test using GraphPad 8.2 (San Diego, CA)

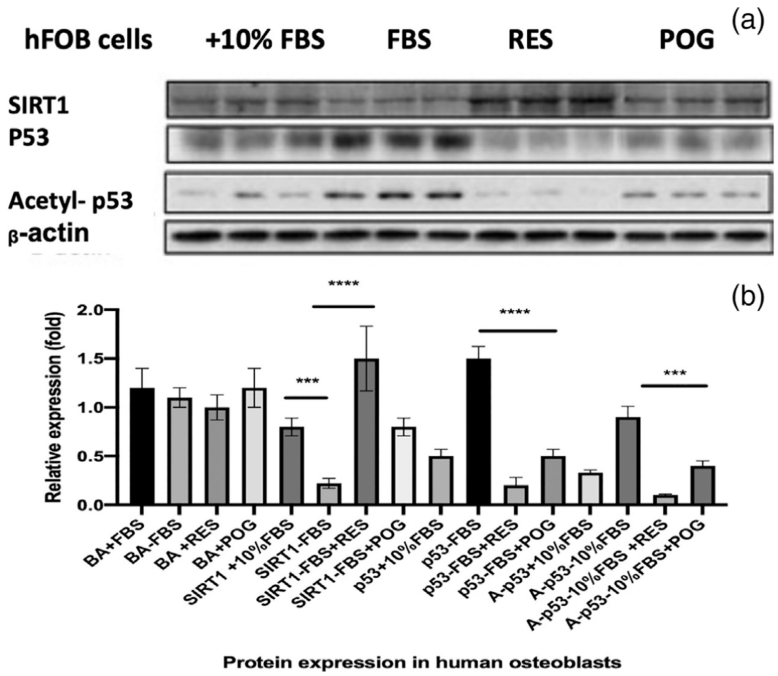

FIGURE 3.

Protein expression levels of SIRT1, p53, and acetylated-p53 from total proteins isolated from control and treated hFOB cells. (a) Total protein was extracted using the Trizol method. The protein expression level of SIRT1, p53, and acetylated-p53 were evaluated by western blot and normalized by β-actin expression rate. The experiments were performed in triplicate. Treatment of the serum-starved (−FBS) cells with resveratrol or peonidin-3-glucoside at 1.0 μg/ml for 72 hr reduced the protein levels of p53 and acetylated-p53 expression. (b) Protein signals were obtained by densitometry and normalized based on total protein concentrations. ***$p < 0.001$; ****$p < 0.0001$. BA = beta-actin. Statistics were performed using one-way ANOVA followed by Dunnett's multiple comparison test using GraphPad 8.2 (San Diego, CA)

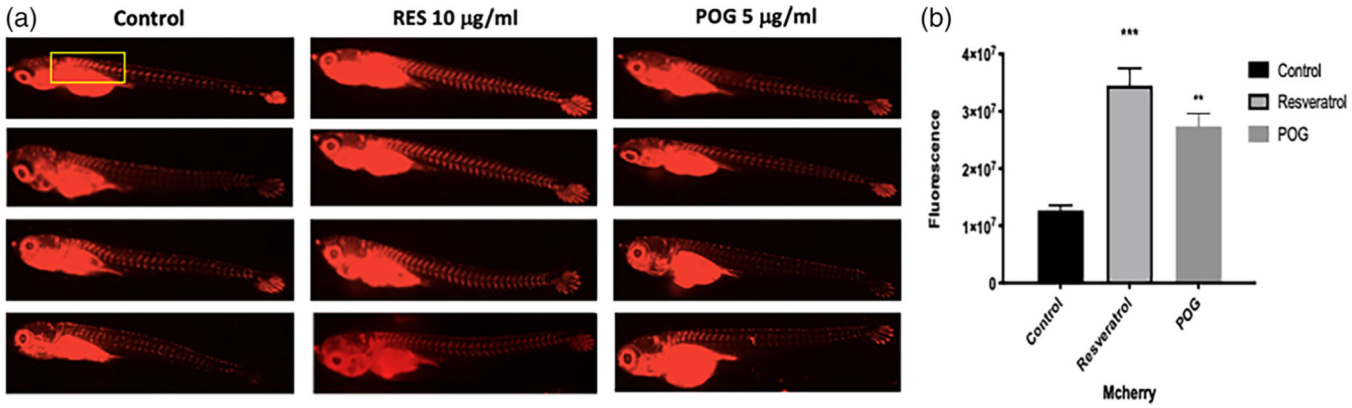

FIGURE 4.

(a) Effects of resveratrol (RES) and peonidin-3-O-glucoside (POG) on the proliferation and differentiation of osteoblasts in *Sp7/osx*: mCherry medaka ($n = 4$ per arm, 9 pdf) at 10 and 5 µg/ml, respectively. Control fish were treated with vehicle solvent only. Transgenic medaka were treated for 5 days after staging, and then viewed using a Keyence fluorescence microscope. Both compounds significantly increased the expression of *Sp7/osx* and *Runx2* as compared with controls (vehicle solvent 0.001% DMSO/water). The improvement in mCherry fluorescence is apparent to the naked eye indicating an increase in *Sp7/osterix* expression and osteoblastogenesis. (b) Graphical analysis of the increased fluorescence. The images were quantitatively analyzed by ImageJ using the ROI (region of interest) manager. Statistics were performed using one-way ANOVA using Graph Pad Prism 8.2, ****$p < 0.0001$, ***$p < 0.001$

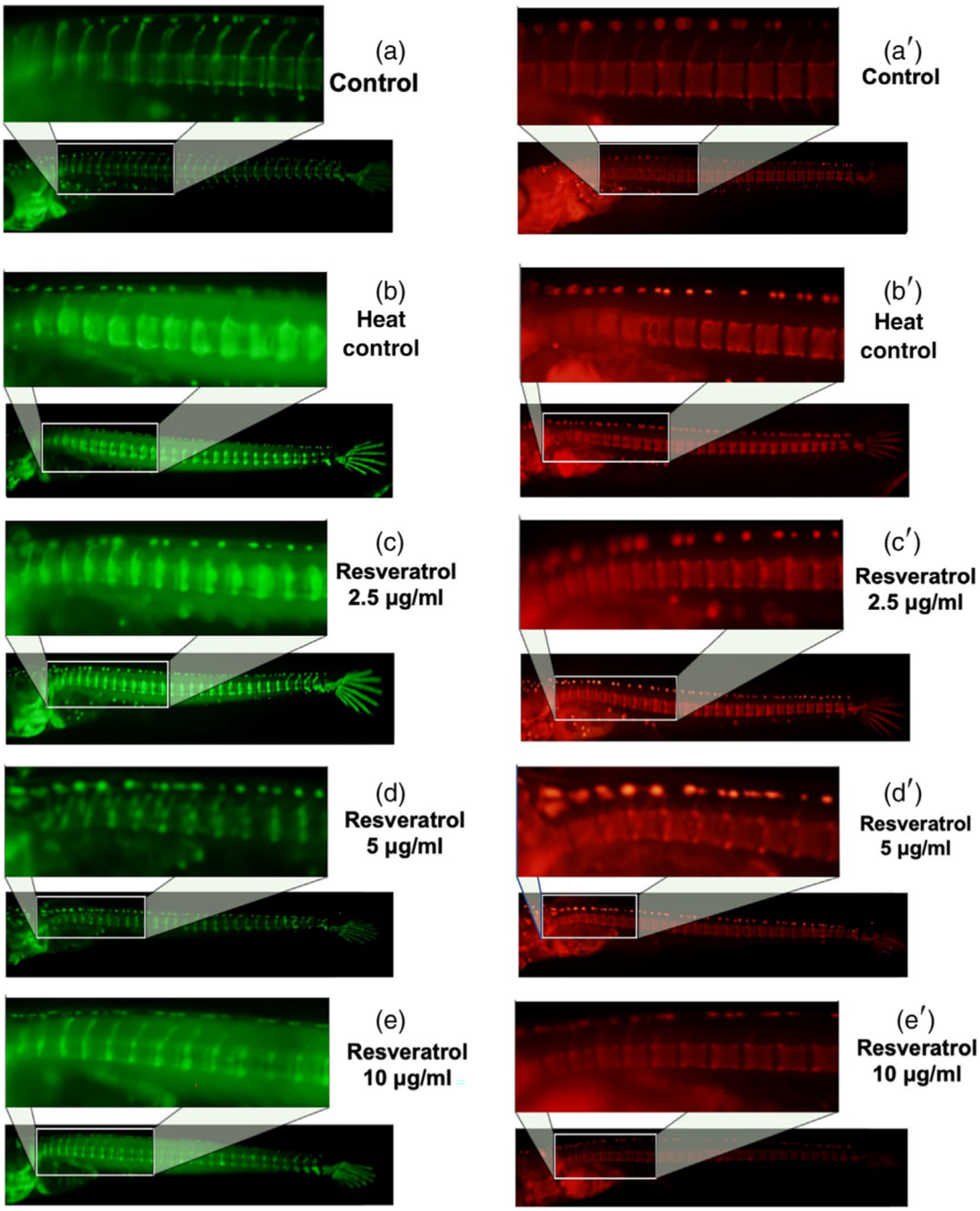

FIGURE 5.

Resveratrol improves bone recovery and reduces resorption in *Col10a1*:mGFP/*Rankl*:HSE:CFP medaka. (a) *Col10a1*:nlGFP expression in *Col10a1*: mGFP/*Rankl*:HSE:CFP larvae at 14 dpf. (b) *Col10a1*:nlGFP expression in *Col10a1*:mGFP/*Rankl*:HSE:CFP medaka at 14 dpf after RANKL induction. (c–e) *Col10a1*: nlGFP expression in *Col10a1*:mGFP/*Rankl*:HSE:CFP larvae at 14 dpf after RANKL induction and resveratrol (2.5, 5 and 10 μg/ml) treatments. (a′) Alizarin complexone (ALC) staining of the mineralized bone matrix at 14 dpf in *Col10a1*:mGFP/*Rankl*:HSE:CFP medaka. (b′)

ALC stained bone matrix at 14 dpf, 5 days after RANKL induction. (c′–e′) ALC stained bone matrix at 14 dpf, 5 days after RANKL induction and treatment

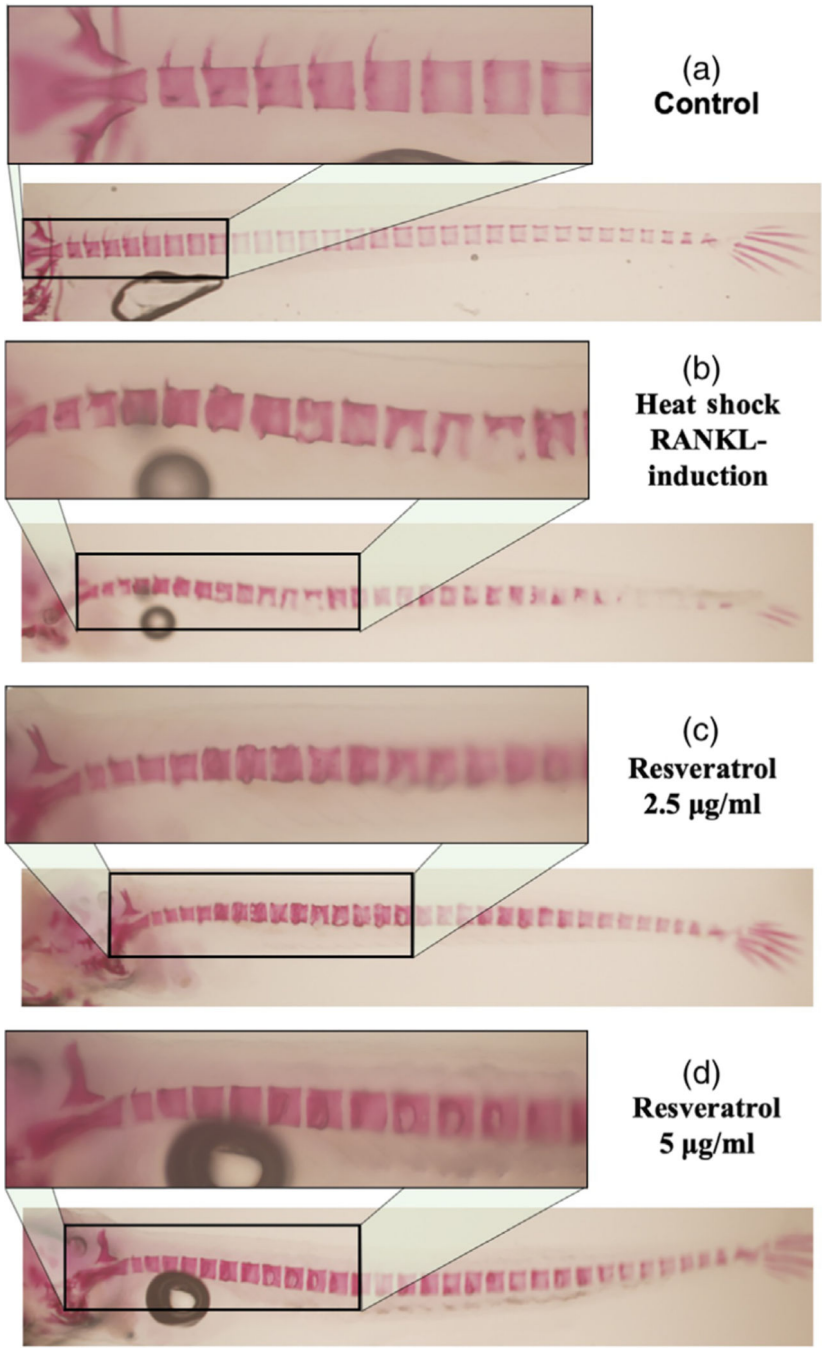

FIGURE 6.

Resveratrol reduces bone resorption after heat-shock induction of rankl:HSE:CFP in medaka larvae. (a) Fixed bone staining with Alizarin Red in *Col10a1*:mGFP/*Rankl*:HSE:CFP medaka larvae at 14 dpf. (b) Fixed bone staining with Alizarin Red in *Col10a1*:mGFP/*Rankl*:HSE:CFP medaka larvae at 14 dpf after RANKL induction. (c,d) Fixed bone staining with Alizarin Red in *Col10a1*:mGFP/*Rankl*:HSE: CFP medaka larvae at 14 dpf. After RANKL induction and resveratrol treatments. Normal centra and arches are observed in

control group. Lesions in centra and arches are observed in the heat-shock RANKL-induced control group. Resveratrol treatments improved centra recovery and reduced bone resorption

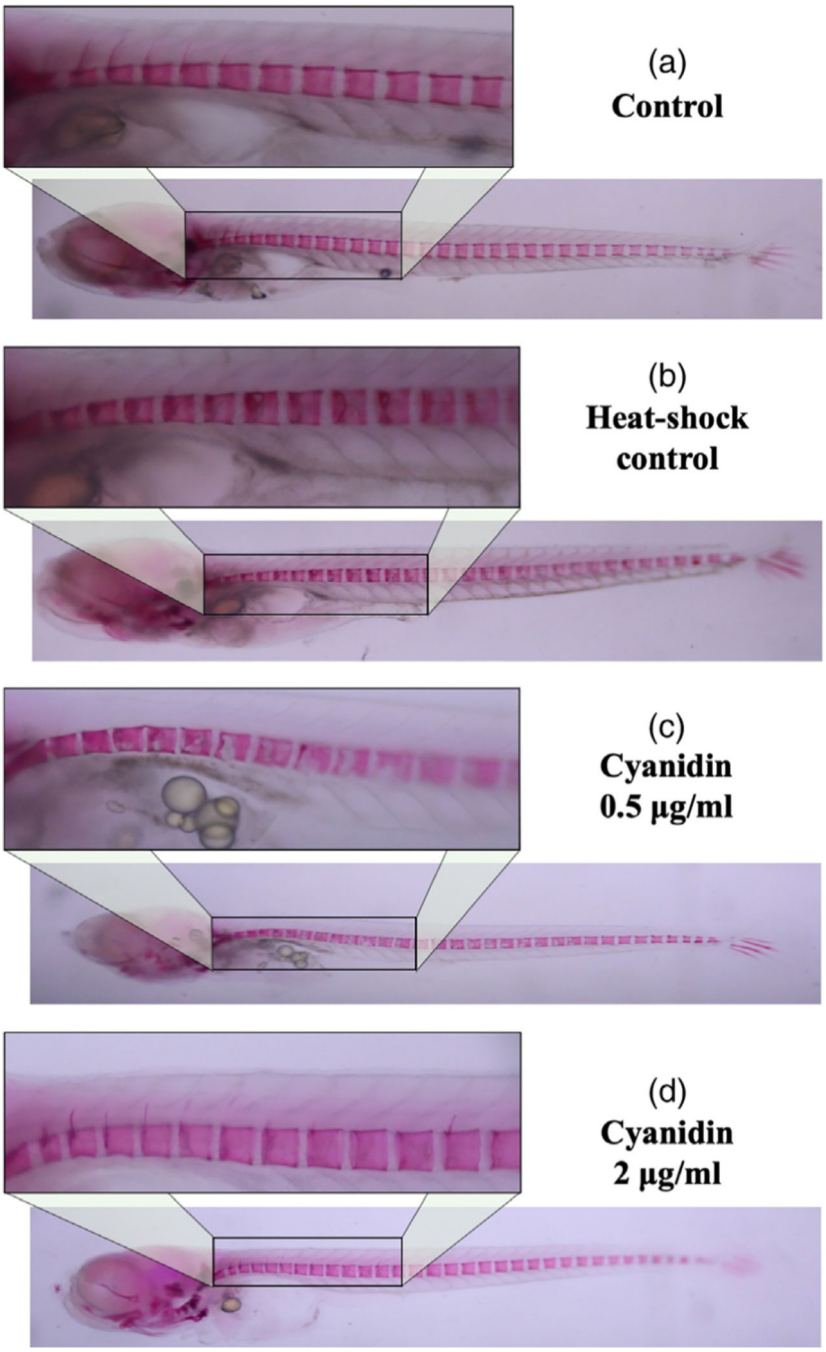

FIGURE 7.

Cyanidin treatments improved bone recovery after heat-shock induction of resorption in *Col10α1*:mGFP/*Rankl*:HSE: CFP Medaka larvae. (a) Fixed bone staining with Alizarin Red in *Col10α1*:mGFP/*Rankl*:HSE:CFP medaka larvae at 14 dpf. (b) Fixed bone staining with Alizarin Red in *Col10α1*:mGFP/*Rankl*:HSE:CFP larvae at 14 dpf after RANKL red after RANKL induction. (c,d) Fixed bone staining with Alizarin Red in *Col10α1*:mGFP/*Rankl*:HSE:CFP larvae at 14 dpf after RANKL induction and treatment with 0.5 and 2.0 µg/ml Cyanidin. 0.5 µg/ml was not effective in reducing heat-shock-induced bone

resorption; however, treatment of the medaka with 2.0 μg/ml of cyanidin reduced mineralized bone matrix degradation by RANKL-induced ectopic osteoclasts by an average of 21%

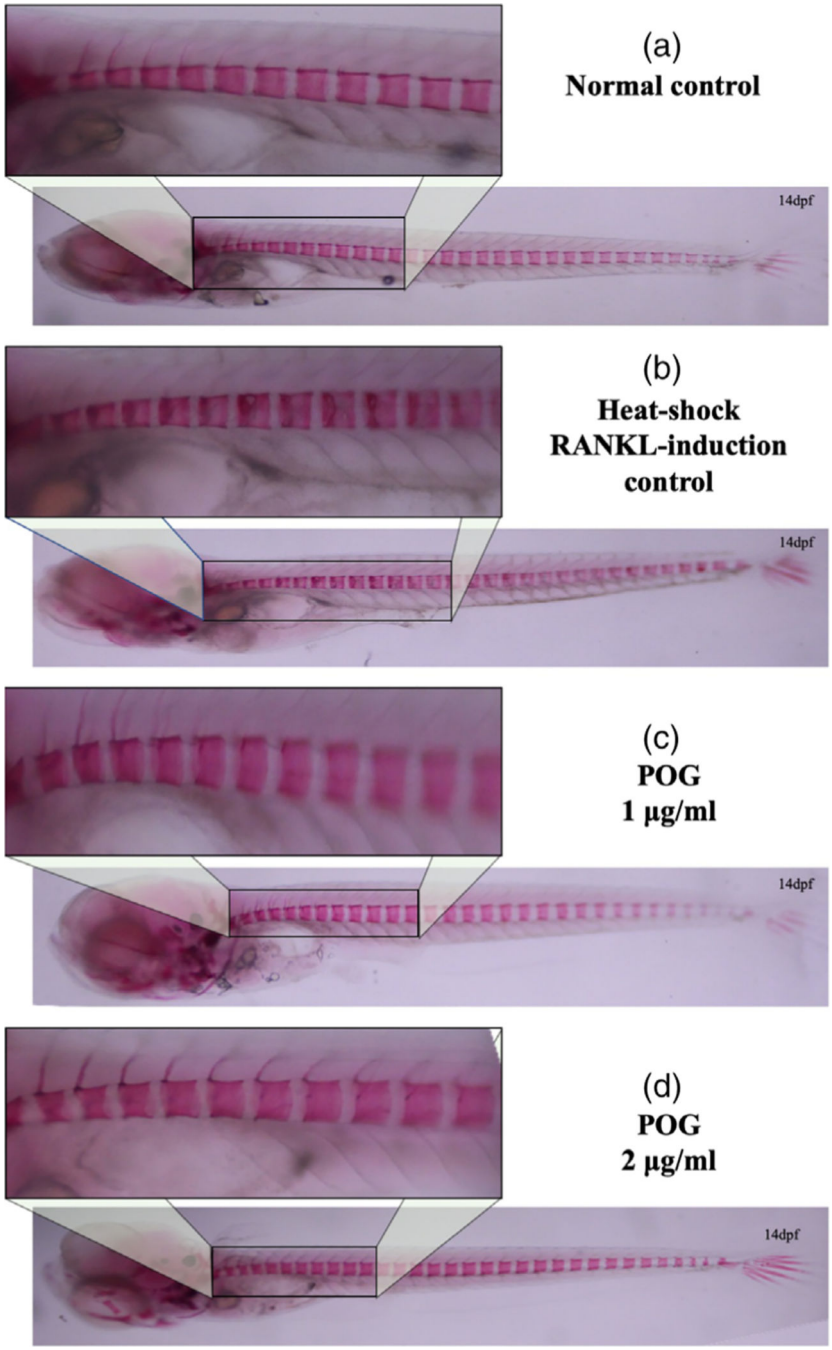

FIGURE 8.

Peonidin-3-O-glucoside (POG) treatments improved bone recovery after heat-shock induction of resorption in *Col10a1*: mGFP/*Rankl*:HSE:CFP medaka larvae. (a) Normal control medaka treated with DMSO 0.01%; Fixed bone staining with Alizarin Red in *Col10a1*:mGFP/*Rankl*:HSE:CFP FP larvae at 14 dpf. (b) Heat-Shock control medaka: Fixed bone staining with Alizarin Red in *Col10a1*: mGFP/*Rankl*:HSE:CFP larvae at 14 dpf after RANKL induction shows a lack of mineralized arches and degradation of the

centra. (c,d) POG treated medaka: Fixed bone staining with Alizarin Red in *Col10a1*:mGFP/*Rankl*:HSE:CFP larvae at 14 dpf after RANKL

Human Gene	Primer Sequences-Forward (S' to 3')	Primer Sequences-Reverse (S' to 3')
Bcl-2	CGCATCAGGAAGGC	AGCTTCCAGACATT
	TAGAGT	CGGAGA
Bax	TGCCAGCAAACTGG	GCACTCCCGCCACA
	TGCTCA	AAGATG
ß-Actin	TGACGTGGACATCC	CTGGAAGGTGGACA
	GCAAAG	GCGAGG
HDAC1	CTACTACGACGGGG	GAGTCATGCGGATT
	ATGTTGG	CGGTGAG
SIRT1	TGCTGGCCTAATAG	CTCAGCGCCATGGA
	AGTGGCA	AAATGT
PGC-1α	GTCGGGCATCCCTG	GGAACCCTGTCTGC
	CCTCAAAGC	CATCACGTCAG
p53	AAGTCTGTGACTTG	GTCATGTGCTGTGA
	CACGTACTCC	CTGCTTGRTAG